

Cytoplasmic Fragment of Alcadin α Generated by Regulated Intramembrane Proteolysis Enhances Amyloid β -Protein Precursor (APP) Transport into the Late Secretory Pathway and Facilitates APP Cleavage*

Received for publication, July 30, 2014, and in revised form, November 14, 2014. Published, JBC Papers in Press, November 18, 2014, DOI 10.1074/jbc.M114.599852

Norio Takei[‡], Yuriko Sobu[‡], Ayano Kimura[‡], Satomi Urano[‡], Yi Piao[‡], Yoichi Araki[‡], Hidenori Taru[‡],
Tohru Yamamoto[§], Saori Hata[‡], Tadashi Nakaya[‡], and Toshiharu Suzuki^{‡1}

From the [‡]Laboratory of Neuroscience, Graduate School of Pharmaceutical Sciences, Hokkaido University, Kita-12 Nishi-6, Kita-ku, Sapporo 060-0812, Japan and [§]Department of Molecular Neurobiology, Faculty of Medicine, Kagawa University, Miki-cho 761-0793, Japan

Background: Alcadin α (Alc α) forms a ternary complex with APP and X11L.

Results: Transport into the nerve terminus and metabolism of APP were facilitated in Alc α CTF transgenic mice, along with an increase in A β .

Conclusion: Alc α ICD, a product of γ -secretase cleavage of Alc α CTF, enhanced APP trafficking from the ternary complex into a late secretory pathway.

Significance: Novel function of Alcadin α results from regulated intramembrane proteolysis.

The neural type I membrane protein Alcadin α (Alc α), is primarily cleaved by amyloid β -protein precursor (APP) α -secretase to generate a membrane-associated carboxyl-terminal fragment (Alc α CTF), which is further cleaved by γ -secretase to secrete p3-Alc α peptides and generate an intracellular cytoplasmic domain fragment (Alc α ICD) in the late secretory pathway. By association with the neural adaptor protein X11L (X11-like), Alc α and APP form a ternary complex that suppresses the cleavage of both Alc α and APP by regulating the transport of these membrane proteins into the late secretory pathway where secretases are active. However, it has not been revealed how Alc α and APP are directed from the ternary complex formed largely in the Golgi into the late secretory pathway to reach a nerve terminus. Using a novel transgenic mouse line expressing excess amounts of human Alc α CTF (hAlc α CTF) in neurons, we found that expression of hAlc α CTF induced excess production of hAlc α ICD, which facilitated APP transport into the nerve terminus and enhanced APP metabolism, including A β generation. *In vitro* cell studies also demonstrated that excess expression of Alc α ICD released both APP and Alc α from the ternary complex. These results indicate that regulated intramembrane proteolysis of Alc α by γ -secretase regulates APP trafficking and the production of A β *in vivo*.

Alcadin (Alc)² is a brain abundant type I membrane protein family comprised of Alc α , Alc β , and Alc γ (1), which are also

identified as the Ca²⁺-binding protein calyculin (2, 3). They share two cadherin repeats, a concanavalin A-like lectin/glucanase superfamily domain in their amino-terminal extracellular region, an acidic domain, a kinesin light chain-binding WD motif and an X11L (X11-like)-binding NP sequence in their carboxyl-terminal cytoplasmic region (1, 4). Originally, we isolated Alc α as an X11L-interacting molecule (1, 5). X11L is a neuron-specific cytoplasmic adaptor protein and was also identified as a binding partner of amyloid β -protein precursor (APP) (6). Both Alc α and APP interact with the phosphotyrosine interaction/phosphotyrosine-binding domain of X11L and form a ternary complex comprised of Alc α , X11L, and APP (1, 5).

In neurons, APP695, a neuron-specific isoform, undergoes N-glycosylation in the endoplasmic reticulum, producing immature APP (7). The immature APP is transported to the Golgi and further modified by O-glycosylation to form mature APP (mAPP). The mAPP enters into the late secretory pathway and localizes to the plasma membrane, whereas some mAPP also enter endosomal recycling pathways. During the late secretory pathway, APP is subject to consecutive cleavages (8). Alc α /calyculin-1 is also subject to intracellular trafficking and metabolism and participates in neural functions, similar to APP (4, 9–11). Calyculinins have also been reported to mediate exit of APP from the TGN (12).

It is well known that APP undergoes primary proteolytic cleavage at juxtamembrane α - or β -sites by α - or β -secretase and that membrane-associated APP C-terminal fragments (APP CTFs) are further cleaved at γ/ϵ -sites by γ -secretase (8). When APP is cleaved by a combination of α - and γ -secretases, a metabolically labile p3 peptide is generated, whereas neuro-

* This work was supported in part by Grants-in-aid for Scientific Research 26293010 (to T. S.) and 24790062 (to S. H.) from the Ministry of Education, Culture, Sports, Science, and Technology in Japan and by Bilateral Joint Research Projects (to S. H.) and an Asian Core Program (to T. S.) of the Japan Society for the Promotion of Science.

¹ To whom correspondence should be addressed. Tel.: 81-11-706-3250; Fax: 81-11-706-4991; E-mail: tsuzuki@pharm.hokudai.ac.jp.

² The abbreviations used are: Alc, Alcadin; APP, amyloid β -protein precursor; CTF, carboxyl-terminal fragment; ICD, intracellular domain fragment; X11L,

X11-like; hAlc, human Alc; A β , amyloid β -protein; mAPP, mature APP(s); Tg, transgenic; DAPT, (3,5-difluorophenylacetyl)-Ala-Phg-OBu; hAlc FL, full-length hAlc; sELISA, sandwich ELISA.

Alc Fragment Regulates APP Trafficking and Metabolism

toxic amyloid β ($A\beta$) peptide is generated when APP is cleaved by β - and γ -secretases. The $A\beta$ peptide is known as a causative molecule of Alzheimer disease (13, 14). $Alc\alpha$ is also subject to proteolytic cleavage by α -secretase and remains a membrane-associated C-terminal fragment ($Alc\alpha$ CTF), which is further cleaved by γ -secretase to secrete p3- $Alc\alpha$ and generate an intracellular domain fragment ($Alc\alpha$ ICD) (10, 15).

X11L associates with both APP and $Alc\alpha$ in the Golgi and also in the late secretory pathway (16, 17). In the Golgi, X11L is thought to regulate the formation of APP and $Alc\alpha$ cargo vesicles (17). Formation of the ternary complex composed of APP, X11L, and $Alc\alpha$ also regulates the entry of APP into lipid rafts where β -secretase is active (16). Additionally, X11L is thought to regulate γ -cleavage of APP CTFs directly (18).

$A\beta$ production is suppressed when APP is expressed with X11L, and we reported that suppressed $A\beta$ production by X11L was further enhanced when full-length $Alc\alpha$ was also coexpressed (1, 5, 6) due to ternary complex formation. *In vitro*, binding of APP to X11L is stabilized when $Alc\alpha$ is coexpressed, and this enhanced interaction of APP with X11L mediated by $Alc\alpha$ is thought to further stabilize APP metabolism as well as regulate intracellular APP trafficking because the cleavage of APP by secretases occurs in the late secretory pathway. *In vivo*, X11L/X11 β transgenic mice expressing human APP suppressed amyloidogenic processing of APP (19). Furthermore, X11L gene knock-out (X11L-KO) mice showed enhanced generation of endogenous $A\beta$ in the brain (20), and human APP transgenic mice lacking the X11L gene exhibited enhanced amyloid plaque formation in the brain (21). However, the role of $Alc\alpha$ metabolites in APP metabolism and $A\beta$ generation remain unclear *in vivo*. To determine the function of $Alc\alpha$ CTF and its intracellular metabolic fragment $Alc\alpha$ ICD, we generated a transgenic mouse line expressing human $Alc\alpha$ -CTF under the control of the PDGF- β promoter and examined its effect on the metabolism of APP *in vivo*.

EXPERIMENTAL PROCEDURES

Generation of hAlc α CTF Transgenic Mouse Lines—cDNA encoding human $Alc\alpha$ CTF (amino acids 817 to 971 of the hAlc α 1 isoform) (1, 10) was connected to the signal sequence (amino acids 1 to 28 of hAlc α 1). The construct was inserted into a vector with a 5'-PDGF- β promoter and a 3'-SV40 poly(A) tail to produce the TgPDhAlc α CTF plasmid. For DNA microinjection, linearized DNA was prepared by digestion with restriction enzymes, as illustrated (see Fig. 1A). Mice were purchased from CLEA-Japan (Tokyo, Japan), and all of the animal studies were conducted in compliance with the guidelines of the Animal Studies Committee of Hokkaido University. Linearized DNA (SalI/NotI fragment) was micro-injected into fertilized eggs produced by mating between BDF1 mice (F1 hybrid of C57BL/6 and DBA/2 mice) according to standard procedures (22). In brief, BDF1 females (6–8 weeks of age) that had been super-ovulated by injection of pregnant mare serum gonadotropin (serotropin, Asuka Pharmaceutical Co.) and human chorionic gonadotropin (Asuka Pharmaceutical Co.) were mated with males of the same strain. Pronuclear stage embryos were collected from pregnant females, and DNA fragments were injected into the male pronuclei of the zygotes. The embryos

were then cultured in potassium simplex optimized medium at 37 °C in an atmosphere of 5% CO₂ and 95% humidity. The surviving embryos were transplanted into the oviducts of pseudo-pregnant females (Multi Cross Hybrid (Institute of Cancer Research), 8–12 weeks of age). Transgenic founders were identified by PCR and Southern blot analysis of genomic DNA extracted from tail biopsies. Genotyping PCR was performed using a set of sense ($Alc\alpha$ CTF, 5'-cct gac cat cac cgt caa cc-3') and antisense (SV40, 5'-cac ctc ccc ctg aac ctg aa-3') primers with ExTaq DNA polymerase (Takara-bio). For Southern blot analysis, genomic DNA was digested with EcoRI, separated by agarose gel electrophoresis, and transferred onto a Nylon membrane. The membrane was incubated with a probe prepared from the DNA sequence of an injected construct, and signals were detected by CDP-Star (GE Healthcare). Founder mice were backcrossed with C57BL/6 mice, and offspring were backcrossed over 10 times. Non-transgenic littermates derived from the same crosses were used as controls.

MALDI-TOF/MS Analysis of p3- $Alc\alpha$ in the Medium of Cells Expressing Human $Alc\alpha$ CTF—Tg construct was recloned into pcDNA3.1 to generate pcDNA3.1-hAlc α CTF. The p3- $Alc\alpha$ peptides secreted into the medium of HEK293 cells transiently transfected with pcDNA3.1-hAlc α CTF was recovered by immunoprecipitation with anti-p3- $Alc\alpha$ UT135 antibody and protein G-Sepharose beads (10). The beads were washed and sample was eluted with trifluoroacetic acid/acetonitrile/water (1:20:20) saturated with sinapinic acid. The dissolved sample was subject to MALDI-TOF/MS analysis with a UltraflexII TOF/TOF (Bruker Daltonics, Bremen, Germany) (10).

Immunohistochemistry—Mouse brain sections (25- μ m thick) were prepared as described (20), and the sections were stored at -30 °C until use. Frozen sections were washed with PBS for 20 min and then incubated in PBS containing 1% (v/v) Triton X-100 for 20 min to permeabilize the membranes. Tissue sections were then incubated with PBS containing 0.3% (v/v) H₂O₂ for 10 min to inactivate endogenous peroxidase activity and washed three times with PBS. The sections were blocked with PBS containing 5% (v/v) normal goat serum for 1 h at room temperature and then incubated with no. 958 antibody (serum diluted to 1:8,000) for ~8 h at 4 °C. After three washes with PBS, sections were incubated with an anti-rabbit IgG peroxidase-linked species-specific whole antibody (GE Healthcare, dilution 1:500) for 30 min at room temperature. The signal was visualized with a VECTASTAIN kit (Vector Laboratories) following the manufacturer's protocol.

Subcellular Fractionation—The cytosolic fraction of mouse brain tissue was prepared as described (23) and subjected to immunoprecipitation with no. 958 antibody. The synaptosome fraction was prepared as described (24) with some modifications. In brief, the cerebral cortex and hippocampus regions of 12-month-old Tg54 and non-Tg mice were homogenized in buffer A (10 mM HEPES (pH 7.4) containing 0.32 M sucrose, 5 μ g/ml chymostatin, and 5 μ g/ml leupeptin), and this fraction was used as total lysate. The lysate was then centrifuged at 1,000 \times g for 10 min, and a clarified supernatant (S1 fraction) was recovered. The S1 fraction was further centrifuged at 13,800 \times g for 20 min, and the supernatant (S2 fraction) and pellet (P2 fraction) were used for assays. The P2 fraction was

suspended again in buffer A and overlaid on a discontinuous sucrose gradient prepared with 1.2 M, 1 M, and 0.85 M sucrose solution and centrifuged at $82,500 \times g$ for 2 h with an SW41 rotor (Beckman Coulter). After centrifugation, the layer between 1.0 M and 1.2 M sucrose was collected and resuspended in 6 mM Tris-HCl (pH 8.0) buffer containing 0.5% (v/v) Triton X-100 to prepare the synaptosome fraction.

Antibodies, Immunoprecipitation, and Immunoblot Analysis—A rabbit polyclonal anti-Alc α carboxyl-terminal domain antibody, no. 958, was raised against a synthesized peptide, ⁹⁴⁸GEQGD⁹⁶²PQNATRQQQL, of human Alc α 1. IgG was affinity purified with antigen-coupled beads and used for analyses. This antibody specifically recognizes Alc α of human and mouse almost equivalently but does not show cross-reactivity with Alc β and Alc γ of human (see Fig. 2A) or mouse (data not shown).

Immunoprecipitation was performed as described (1) using a previously described plasmid for FLAG-X11L (6). For the APP-GFP construct, human APP695 cDNA was cloned into pEGFP-N3 (Clontech) between the HindIII/NotI sites. For the hAlc α ICD construct, cDNA encoding the cytoplasmic region of hAlc α from 868 to 971 amino acids was cloned into pcDNA3.1. Amino acid position 868 of Alc α 1 is the major N terminus of Alc α ICD, which is generated by ϵ -cleavage of Alc α CTF by γ -secretase (15). Brain and cell extracts used in immunoblot analyses were prepared by homogenizing samples in eight volumes of RIPA buffer containing 5 μ g/ml chymostatin and 5 μ g/ml leupeptin. The lysates were centrifuged, and supernatants were used for immunoprecipitation analysis. The procedures used for immunoblotting and the identification of APP CTFs were described previously (25).

Antibodies used in immunoblot analysis were as follows: rabbit polyclonal anti-Alc α (no. 958) and anti-APP (no. 8717, Sigma), mouse monoclonal anti-FLAG (M2, Sigma), anti-flotillin-1 (BD Biosciences), anti-synaptophysin (SY38, DAKO), anti- α -tubulin (sc-32293, Santa Cruz Biotechnology), anti-GM130 (BD Biosciences), anti-GFP (no. 598, MBL), and anti- β -actin (ab8226, Abcam). For quantification of immunoreactive proteins, a VersaDoc system (Bio-Rad) or LAS-4000 mini (Fujifilm) was used. The intensities of the protein bands of Alc α CTF, APP full-length, and APP CTFs were normalized to the values of flotillin-1.

sELISA for Quantification of Mouse A β and p3-Alc α —To quantify A β in mice brains, the cerebral cortex and hippocampus were excised from 12- to 15-month-old mice, and TBS-soluble and -insoluble fractions were prepared as described (16). Mouse A β ^{1–40} and A β ^{1–42} in the TBS-soluble and -insoluble fractions were examined with an sELISA kit (A β ^{1–40}, no. 27720; A β ^{1–42}, no. 27721; IBL, Takasaki, Japan). Quantification of p3-Alc α was described previously (26).

Immunofluorescence Microscopy Analysis and Quantification of Fluorescence Intensity—The procedures in immunofluorescence experiments shown in Fig. 5 were followed as described previously (27). The images were analyzed by a fluorescence microscope (Keyence, BZ-700X). Fluorescence quantification was performed using the imaging software ImageJ (<http://imagej.nih.gov/ij/>, National Institutes of Health). The images were acquired with a resolution of 640 \times 480 pixels

using a 100 \times objective lens, which covered the whole cell region. The region of interest that contained the cell body-neurite junction area was selected at a resolution of 132 \times 48 pixels, in which the junction was set to a middle region manually using a transparent image obtained by transmission light. The fluorescence intensities in the proximal region of neurite (“neurite,” right half of a selected image) and the hillock of cell body (“cell body,” left half of a selected image) were then measured. The fluorescence intensities where no cell region was observed in the right and left half images were also measured as background. The background intensity was subtracted from the respective intensity of cell body and neurite, and the values were indicated as a ratio to average intensity of neurite plus cell body.

RESULTS

Generation of Human Alc α Carboxyl-terminal Fragment Transgenic Mice—A cDNA sequence encoding the carboxyl-terminal region of human Alc α 1 together with the signal peptide sequence was expressed under the regulation of the mouse PDGF- β promoter (Fig. 1A). The signal sequence was cleaved correctly by signal peptidase when expressed in HEK293 cells, producing the human Alc α carboxyl-terminal fragment (hAlc α CTF) with the correct amino-terminal sequence. hAlc α CTF then underwent intramembrane cleavage by γ -secretase to generate p3-Alc α with the same amino acid sequence observed *in vivo* (10). MALDI-TOF/MS analysis of p3-Alc α secreted from HEK293 cells showed that the p3-Alc α 35 (amino acid sequence indicated in B) was generated as a major p3-Alc α form along with several minor species (Fig. 1B). The result indicates that exogenously expressed hAlc α CTF was processed in a manner similar to that of endogenously generated Alc α CTF.

We generated six transgenic mouse founder lines using this construct (Fig. 1C). Genomic Southern blot analysis of the six lines shows a few to several hundred copies of exogenous gene incorporated into the genome (Fig. 1D). The protein expression level of hAlc α CTF in the brain region, including the cerebral cortex and hippocampus was analyzed in the three lines with the highest trans-gene dose by immunoblotting with an anti-Alc α antibody (Fig. 1E). Of these founders, line no. 54, which showed a 4-fold increase in hAlc α CTF expression compared with endogenous levels of the protein, was chosen for use in further analyses. Tg54 was subjected to genetic back-cross with C57BL/6 over 10 generations.

Expression of hAlc α CTF in Tg54 Mouse Brain—Alcadin family proteins Alc α , Alc β , and Alc γ share a similar structure in the cytoplasmic region. Therefore, we developed an antibody raised against the cytoplasmic sequence of Alc α . This antibody, designated no. 958, recognizes specifically Alc α and its CTF but not Alc β or Alc γ . An anti-FLAG antibody was used to confirm the levels of expression in cells expressing these FLAG-tagged constructs (Fig. 2A).

Using this antibody, we analyzed the expression of hAlc α CTF in 3-month-old Tg54 (Tg) and non-Tg (N) mice (Fig. 2, B and C). Under the regulation of the PDGF- β promoter, increased expression of hAlc α CTF was observed in the cerebral cortex, hippocampus, and olfactory bulb in Tg compared with non-Tg mice (Fig. 2B). Immunohistochemical analysis of

Alc Fragment Regulates APP Trafficking and Metabolism

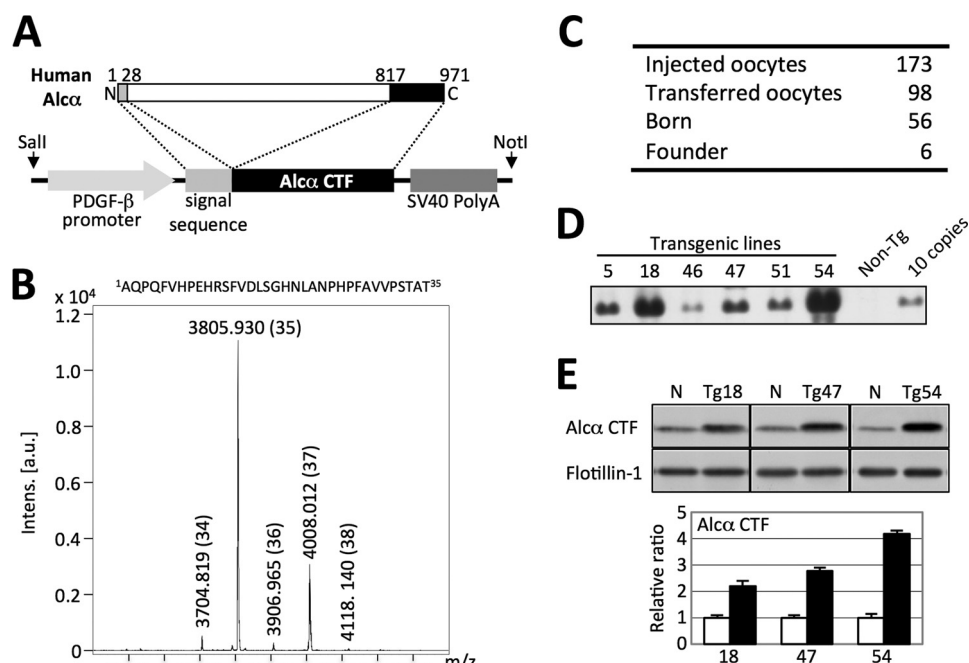


FIGURE 1. Generation and characterization of hAlc α CTF transgenic mouse lines. *A*, construct for generation of hAlc α CTF transgenic mouse lines. The cDNA sequence encoding amino acids 817–971 of human Alc α 1 (971 amino acids) was ligated with cDNA encoding the signal sequence (amino acids 1 to 28) and cloned into a vector with the 5'-PDGF- β promoter sequence and 3'-SV40 poly(A) sequence. DNA fragments prepared by digestion with Sall and NotI were used for injection into fertilized eggs. *B*, identification of human p3-Alc α secreted from HEK293 cells expressing hAlc α CTF. Amino acid sequence of human p3-Alc α 35 and a representative MS spectrum of immunoprecipitate recovered from medium of HEK293 cells expressing human Alc α CTF with anti-p3-Alc α antibody UT135 are shown. Numbers in parentheses indicate p3-Alc α species (35 indicates p3-Alc α 35, a major p3-Alc α species). *Intens.*, Intensity; *a.u.*, arbitrary unit. *C*, establishment of hAlc α CTF Tg mouse founders. A summary of the individual numbers at the respective experimental stages is shown. *D*, genomic Southern blot analysis of six transgenic lines. Genomic DNA of six founders was analyzed by Southern blotting with DNA fragments prepared by Sall/NotI digestion (*A*) as a probe. The transgenic lines used are numbered, along with non-transgenic mouse (Non-Tg) DNA and 10 copies of injected DNA. *E*, expression levels of hAlc α CTF in three Tg mice lines. Protein expression of hAlc α CTF, a transgenic product, was quantified by immunoblotting. A brain region, including the cerebral cortex and hippocampus of Tg18, Tg47, and Tg54 mice along with their non-Tg littermates (N), was lysed and analyzed by immunoblotting with anti-Alc α no. 958 (*top*) and anti-flotillin-1 (*bottom*) antibodies. Band densities of Alc α CTF were quantified and standardized with respect to the band density of flotillin-1. Expression levels in Tg mice (*filled bars*) are shown as a ratio relative to the endogenous Alc α CTF level of non-Tg littermates (*open bars*), which was set at 1.0. Data represent mean \pm S.E. ($n = 3$). Specificity of the anti-Alc α no. 958 antibody is shown in Fig. 2*A*.

endogenous Alc α and hAlc α CTF expression agreed well with the results of immunoblot analysis. An immuno-reactive signal was observed throughout the cerebral cortex (Fig. 2*C*, panels *a* and *d*), in pyramidal cells in CA1 to CA3 along with granule cells in the dentate gyrus of the hippocampus (Fig. 2*C*, panels *b* and *e*), and in layers of mitral and granule cells of the olfactory bulb (Fig. 2*C*, panels *c* and *f*). These signals were enhanced in Tg54 mouse brains (Fig. 2*C*, panels *d*–*f*). Immunoreactivity of tissue staining is specific because this antibody does not react to the tissue staining of Alc α -KO mouse brain (data not shown). Taken together, we concluded that the Tg line expressing hAlc α CTF, Tg54, was successfully established. Tg54 mice exhibit normal growth and fertility (data not shown).

We next measured the amounts of p3-Alc α , which is generated by γ -secretase cleavage of Alc α CTF (illustrated in Fig. 2*F*). In brains of Tg54 mice, the total amount of p3-Alc α greatly increased, whereas in non-Tg mice, it was below the level of detection (Tg, 0.33 ± 0.03 pmol/g tissue; $n = 3$, Fig. 2*D*). Corresponding to the increased amount of p3-Alc α in brain tissue, a significant amount of hAlc α ICD, which was detected as a doublet, was also detected in the cytosolic fraction of Tg54 mouse brain tissue, whereas only very low levels were detected in non-Tg mice (Fig. 2*E*). These findings indicate that exogenously expressed hAlc α CTF is physiologically cleaved by

γ -secretase in the brain to generate p3-Alc α along with Alc α ICD (10, 15).

Facilitation of Intracellular Trafficking and Metabolism of Endogenous Mouse APP in Tg54 Mice—To reveal the effect of Alc α CTF on the metabolism of APP *in vivo*, the amounts of endogenous A β ^{1–40} and A β ^{1–42} in brain lysate isolated from the cerebral cortex and hippocampus were quantified in 12- to 15-month-old Tg54 and non-Tg mice. Unexpectedly, the amounts of both A β species were significantly greater in Tg54 than non-Tg mice (TBS insoluble A β ^{1–40}, non-Tg = 0.61 ± 0.04 pmol/g tissue; Tg54 = 0.72 ± 0.02 pmol/g tissue ($p = 0.0017$); TBS insoluble A β ^{1–42}, non-Tg = 0.18 ± 0.00 pmol/g tissue, Tg54 = 0.22 ± 0.01 pmol/g tissue ($p = 0.0105$)) (Fig. 3*A*). The amount of A β yielded in the TBS-soluble fraction was too small to detect a significant change. These results suggest that the metabolism of APP is facilitated in the brains of Tg54 mice.

Cleavage of APP in neurons occurs during or after its axonal transport; in other words, in the late secretory pathway. Therefore, the brains of Tg54 and non-Tg mice were fractionated to isolate the synaptosome fraction, which includes membrane vesicles of the late secretory pathway. As shown in Fig. 3*B*, the amounts of full-length APP, especially mAPP in synaptosomes, was significantly greater in Tg54 mice (synaptosome = 1.24 ± 0.19 ($n = 5$, $p = 0.0458$) when the value in non-Tg mice was set

Alc Fragment Regulates APP Trafficking and Metabolism

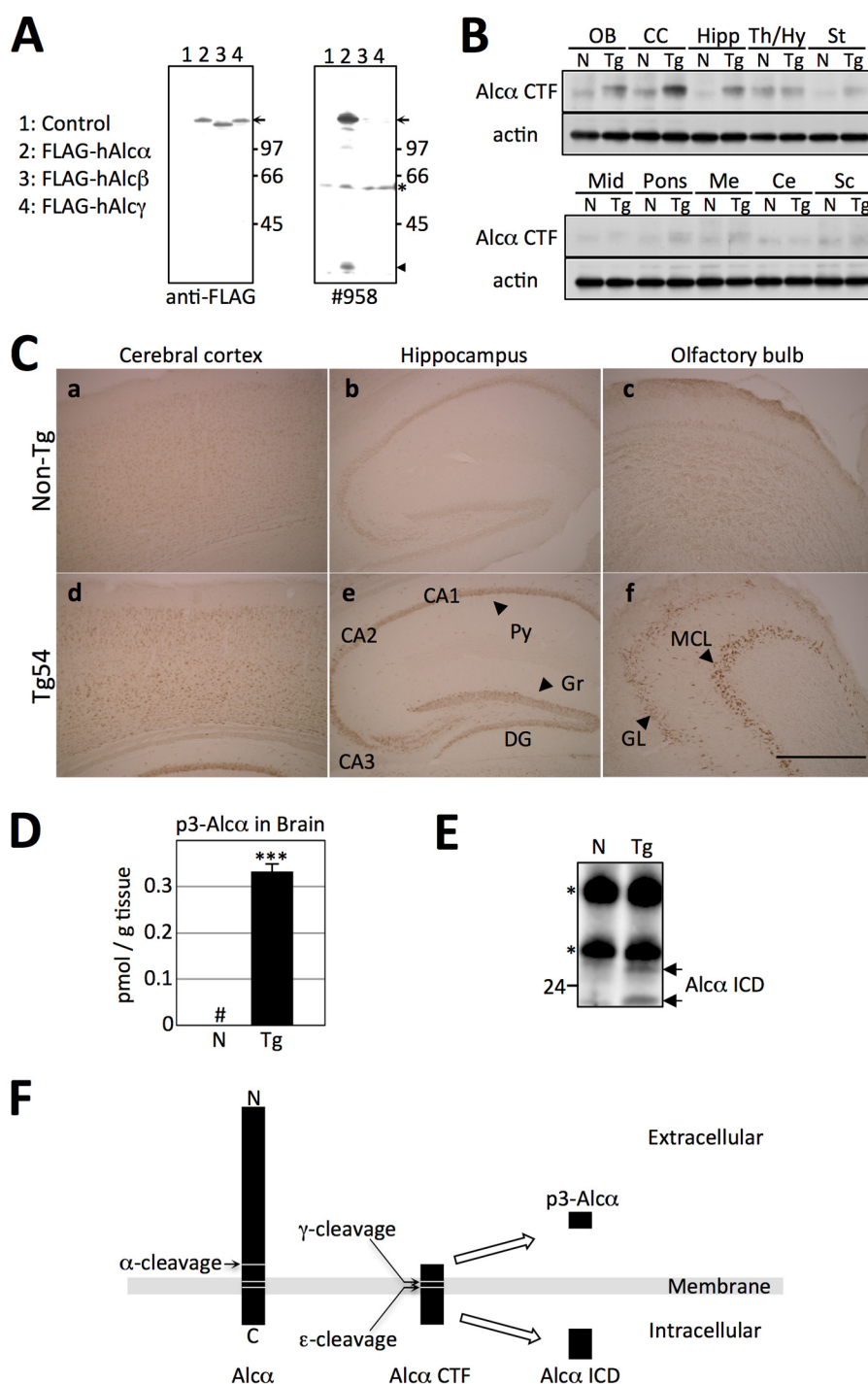


FIGURE 2. Expression of hAlc α CTF in the brains of Tg54 mice. *A*, specificity of anti-Alc α carboxyl-terminal domain antibody no. 958. Lysates of HEK293 cells expressing human FLAG-Alc α (lane 2), human FLAG-Alc β (lane 3), and human FLAG-Alc γ (lane 4) along with plasmid alone (lane 1) were analyzed by immunoblotting with anti-FLAG M2 (left) and anti-Alc α no. 958 (right) antibodies. The arrow indicates FLAG-tagged Alc α , Alc β , and Alc γ , and the arrowhead indicates Alc α CTF. Numbers indicate protein standards (kDa). The asterisk indicates a nonspecific product. *B*, expression of hAlc α CTF in the brain regions of Tg54 mice. Expression of hAlc α CTF in brain regions of Tg54 mice was examined by immunoblotting with no. 958 antibody. Brain tissue from 3-month-old Tg54 (Tg) and non-Tg (N) littermates were dissected into the indicated brain regions, and lysates obtained from these sections were analyzed by immunoblotting with no. 958 (top) and anti- β -actin (bottom) antibodies. OB, olfactory bulb; CC, cerebral cortex; Hipp, hippocampus; Th/Hy, thalamus/hypothalamus; St, striatum; Mid, midbrain; Me, medulla; Ce, cerebellum; Sc, spinal cord. *C*, localization of hAlc α CTF in the brains of Tg54 mice. Localization of hAlc α CTF in brain regions was examined by immunostaining with no. 958 antibody. Sections of the cerebral cortex (*a* and *d*), hippocampus (*b* and *e*), and olfactory bulb (*c* and *f*) were prepared from 3-month-old Tg54 (*d–f*) and non-Tg (*a–c*) littermates and immunostained. Py, pyramidal cells; Gr, granule cells; DG, dentate gyrus; MCL, mitral cell layer; GL, granule cell layer. *D*, quantification of p3-Alc α in the brains of Tg54 mice. The total amount of p3-Alc α in the brains of 6-month-old Tg54 (Tg, filled bar) and non-Tg (N, open bar) littermates were quantified by sELISA. Quantified values are given as the mean \pm S.E. ($n = 4$). ***, $p < 0.005$, Student's *t* test. #, below detectable levels. *E*, detection of hAlc α ICD in the cytosolic fraction of mice brains. Brain lysates prepared from 2-month-old Tg54 (Tg) and non-Tg (N) mice brains were subjected to immunoprecipitation with no. 958 antibody, and the precipitates were detected by immunoblotting with the same antibody. Arrows indicate hAlc α ICD fragments. Numbers on the left side of the panel indicate the molecular mass (kDa). Asterisks indicate IgG heavy and light chains. *F*, schematic structure of p3-Alc α and hAlc α ICD. Alc α CTF is first cleaved at the ϵ -site by γ -secretase to release Alc α ICD into the cytoplasm. Next, γ -secretase cleavages reach to the γ -site to secrete p3-Alc α into the extracellular milieu (15).

Alc Fragment Regulates APP Trafficking and Metabolism

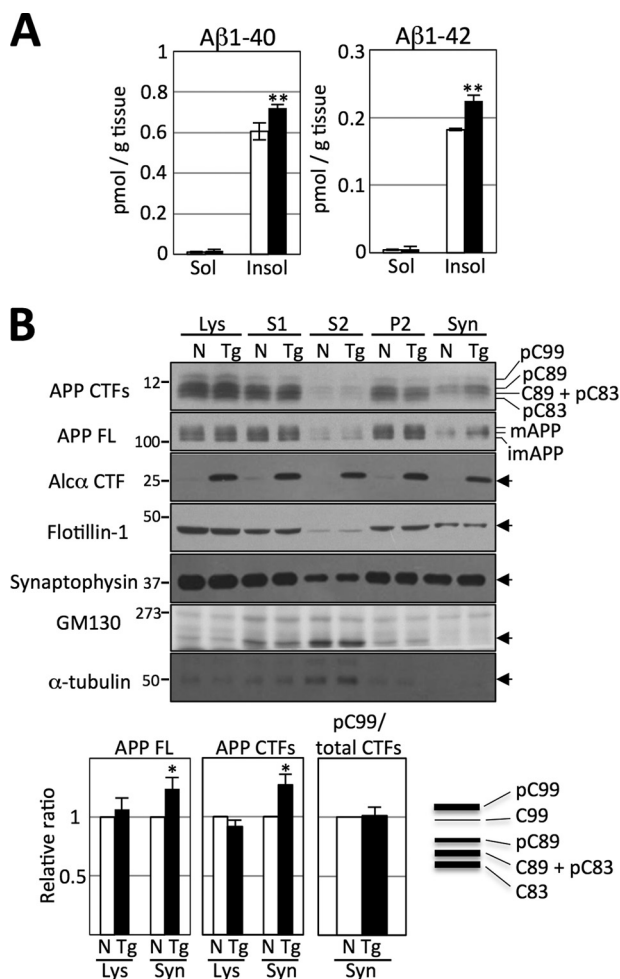


FIGURE 3. Changes in APP metabolism in the brains of Tg54 mice. A, quantification of Aβ¹⁻⁴⁰ and Aβ¹⁻⁴² in brain tissue of Tg54 and non-Tg mice. Brain regions, including the cerebral cortex and hippocampus of 12- to 15-month-old Tg54 (filled bars) and non-Tg (open bars) mice, were dissected, and endogenous Aβ¹⁻⁴⁰ (left) and Aβ¹⁻⁴² (right) in the TBS-soluble and -insoluble fractions were quantified by sELISA. Results are given as the means ± S.E. Asterisks indicate statistical significance as determined by Student's *t* test ($n = 12$, **, $p < 0.01$). B, subcellular localization of APP and APP CTFs in Tg54 and non-Tg brains. Brain regions, including the cerebral cortex and hippocampus of 12-month-old Tg54 (Tg) and non-Tg (N) littermates, were fractionated and analyzed by immunoblotting with antibodies against the indicated proteins: anti-APP (no. 8717, Sigma) for APP CTFs and APP FL, anti-Alcα (no. 958) for Alcα CTF, anti-flotillin-1 (BD Biosciences), anti-synaptophysin (SY38, DAKO), anti-GM130 (BD Biosciences), and anti-α-tubulin (sc-32293, Santa Cruz Biotechnology). Full-length APP (APP FL), mature (mAPP with *N*- and *O*-glycosylation) and immature (*imAPP* with *N*-glycosylation) APP695 are indicated. C99 and C89 indicate CTFβ, and C83 indicates CTFα. The pC99, pC89, and pC83 are CTFs phosphorylated at Thr-668. (A schematic blot of detected CTFs is indicated in the lower right panel.) Lys, total lysate; S1, post-nuclear supernatant; S2 and P2, supernatant and pellet of S1 fraction that was subjected to further centrifugation; Syn, synaptosome fraction. Numbers on the left represent protein molecular mass standards. Arrows on the right indicate the protein detected with antibodies. The bar graphs show the results of quantification of protein bands in the total lysate (Lys) and synaptosome fractions (Syn). Quantified values of APP FL (far left graph) and APP CTFs (middle graph) in the lysate and synaptosome fractions are indicated. The pC99 was also quantified, and the ratio of pC99/total CTFs (right graph) is shown. Values were normalized to the values of flotillin-1. Values obtained from non-Tg mice were set to 1.0 and are given as the mean ± S.E. Asterisks indicate statistical significance as determined by Student's *t* test ($n = 5$; *, $p < 0.05$).

at 1.0). However, total APP, which includes mAPP and immature APP, was not changed significantly in the total lysate of either Tg or non-Tg mice (lysate = 1.06 ± 0.19 , $n = 5$, $p = 0.4904$). APP CTFs were also significantly more abundant in the

synaptosome fraction of Tg54 mice compared with non-Tg mice (1.27 ± 0.09 ($n = 7$, $p = 0.0261$) when the value in non-Tg mice was set at 1.0), whereas the amounts were equivalent in total lysate of Tg54 and non-Tg mice (0.92 ± 0.05 , $n = 7$, $p = 0.1843$). These results suggest that increased amounts of APP undergo enhanced trafficking into the nerve terminus where it is cleaved by primary secretases. Increased CTFs in the late secretory pathway are then further cleaved by γ-secretase in Tg54 mice, thus facilitating the production of Aβ in the brain. This is not the result of enhanced amyloidogenic processing of APP. Aβ^{1-40/1-42} is derived from C99 among three CTF species; C99 (CTFβ), C89 (CTFβ), and C83 (CTFα). These CTFs are phosphorylated at Thr-668 in brain, and the phosphorylated C99 (pC99) is a major C99 rather than non-phosphorylated form in mouse brain (7). Therefore, an increase of pC99 level can indicate the enhanced amyloidogenic cleavage of APP. However, in Fig. 3B, the ratio of pC99 to total CTF was equivalent in the synaptosome fraction of Tg54 and non-Tg mice brains, although total amounts of APP CTFs increased significantly in the synaptosome fraction of Tg54. Therefore, we understand that the increased Aβ production in Tg54 is due to the facilitated trafficking of APP into the late secretory pathway rather than the enhanced amyloidogenic cleavage of APP. Identification of mature and immature APP and APP CTF species in the brain was described in detail previously (7).

We then considered the possibility that hAlcα ICD derived from hAlcα CTF could play a role in processing the increased amounts of APP entering the late secretory pathway, because the hAlcα ICD was free from membrane association and highly abundant in Tg54 (Fig. 2F). APP and Alcα are associated in the Golgi apparatus via interaction with X11 family proteins. Interaction of APP with X11L, a neuron-specific protein, is enhanced by association of Alcα with X11L. APP in this ternary complex is thought to suppress further trafficking into the late secretory pathway, thus stabilizing APP for cleavage by secretases. In Tg54 mice, excess expression of hAlcα CTF is likely to relieve this suppression. hAlcα CTF is then quickly cleaved by γ-secretase to generate hAlcα ICD along with p3-Alcα (Fig. 2, D–E). Thus, hAlcα ICD could perform a function different from full-length Alcα in stabilizing APP metabolism in the presence of X11L.

To assess this possibility, hAlcα ICD was coexpressed in Neuro2a cells, together with GFP-tagged hAPP (hAPP-GFP), full-length hAlcα (hAlcα FL), and FLAG-tagged X11L (FLAG-X11L), which form a ternary complex (Fig. 4). In the absence of hAlcα ICD, co-immunoprecipitation with an anti-FLAG antibody recovered FLAG-X11L together with hAPP-GFP and hAlcα FL (Fig. 4A, lane 5). However, increased expression of hAlcα ICD decreased the recovery of both hAPP-GFP and hAlcα FL significantly (Fig. 4A, lanes 6–8, and 4B), although hAPP-GFP, hAlcα FL, and FLAG-X11L are expressed at equal levels (Fig. 4A, lanes 1–4). These results indicate that Alcα ICD performs a novel function that releases both APP and Alcα from X11L and is different from the function of Alcα FL. Thus, it is possible to conclude that the increased levels of APP and its metabolic fragments APP CTFs and Aβ in the synaptosome fraction of the brains of Tg54 mice is due to enhanced release and anterograde trafficking of APP to the nerve terminus from

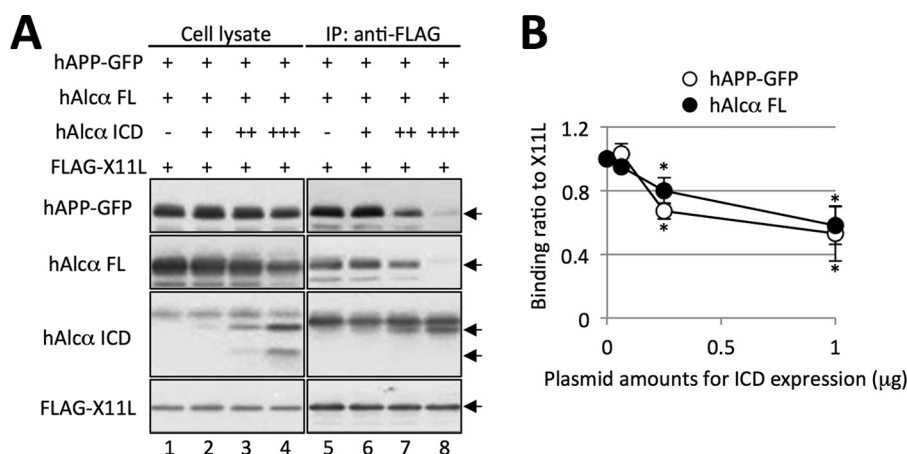


FIGURE 4. Facilitation of APP and Alc α release from the APP/X11L/Alc α ternary complex by Alc α ICD. *A*, co-immunoprecipitation of ternary complex components in the presence of hAlc α ICD. Neuro2a cells expressing human APP-GFP (hAPP-GFP), full-length Alc α (Alc α FL), and FLAG-X11L with or without hAlc α ICD were analyzed for formation of a ternary complex composed of APP, X11L, and Alc α . Proteins in cell lysates (lanes 1–4) were subjected to immunoprecipitation with anti-FLAG antibody and co-immunoprecipitated proteins (IP) were analyzed by immunoblotting with antibodies (lanes 5–8); anti-GFP (no. 598, MBL), anti-Alc α (UT83) (see Ref. 1) and anti-FLAG (M2, Sigma). *B*, quantification of APP and Alc α recovered by co-immunoprecipitation assay. Protein band densities of hAPP-GFP (open circle) and hAlc α FL (filled circle) co-immunoprecipitated with FLAG-X11L were quantified and are shown relative to the value obtained in the absence of hAlc α ICD expression (0, set to 1.0). The horizontal axis represents the amount of pcDNA3-hAlc α ICD (μg) co-transfected with pcDNA3-hAPP-GFP (1 μg), pcDNA3-hAlc α (1 μg), and pcDNA3-FLAG-X11L (0.5 μg). Results are given as the means \pm S.E. Asterisks indicate statistical significance as determined by Student's *t* test ($n = 3$; *, $p < 0.05$).

the cell body. In summary, Alc α ICD regulates the trafficking of APP and Alc α itself. This may be a novel function involved in regulated intramembrane proteolysis by γ -secretase (28, 29).

Alc α ICD Regulates the Trafficking of APP into Neurites—To analyze the function of Alc α ICD on the trafficking of APP into neurites, we used Neuro2a cells that exhibit the extensions of neurites under a normal culture condition. In neuronal cells expressing EGFP-APP, APP appears the proximal region of extending neurites because APP is subject to an anterograde transport into the late secretory pathway (4). Therefore, we analyzed quantitatively the fluorescence signals of EGFP-APP in the proximal region of neurites (Fig. 5).

When Alc α CTF was expressed in Neuro2a cells expressing EGFP-APP and HA-X11L, fluorescence signal of APP appears in the proximal neurite, whereas the signal reduced significantly in the presence of 10 mM DAPT (γ -secretase inhibitor: (3,5-difluorophenylacetyl)-Ala-Phg-OBu^t) (Fig. 5, *B* and *C*, upper panels). Cells treated with DAPT showed the increased Alc α CTF levels (Fig. 5*D*), suggesting the production of Alc α ICD by γ -secretase cleavage of Alc α CTF was inhibited.

When Alc α ICD was further expressed in the cells along with Alc α CTF expression, EGFP-APP fluorescence in the proximal region was not decreased by DAPT treatment (Fig. 5, *B* and *C*, lower panels). These observations indicate that Alc α ICD, but not Alc α CTF, facilitates the trafficking of APP into the late secretory pathway.

DISCUSSION

Because it was documented that the generation of A β from APP and the formation of neurotoxic A β oligomers in neurons are closely linked to the etiology of Alzheimer disease, many efforts have been made to identify the modulator of APP metabolism, including A β generation and clearance (14). With regard to APP trafficking and metabolism, we and others have reported previously that X11 family proteins (X11s) are regulators of APP metabolism (6, 16, 20, 30–33). Excess expression of

X11s suppresses APP processing, including A β generation and APP trafficking, via binding of X11L to APP. Furthermore, X11s function in the regulation of γ -cleavage of APP CTF directly or indirectly (18) or of β -cleavage of APP indirectly (16). Importantly, X11s-KO mice showed a significant increase in endogenous A β generation in the brain and increased formation of amyloid plaques was observed in the brains of hAPP-Tg/X11s-defective mice, indicating that X11s play an important role in APP regulation at various stages of APP metabolism and trafficking *in vivo* (16, 20, 21, 34, 35).

This effect is further enhanced in the presence of Alc α by the formation of a metabolically stable ternary APP·X11L·Alc α complex. This suggests that along with X11L, Alc α may be a key molecule for APP metabolism and trafficking *in vivo*. Because our previous *in vitro* study indicated that not only Alc α , but also Alc α CTF, could form a ternary complex together with X11L and APP in cultured cells (1), we hypothesized that membrane-associated full-length Alc α and Alc α CTF would suppress the production of A β in the presence of X11L.

However, we observed that the brains of Tg54 mice expressing excess amounts of hAlc α CTF showed a significant increase in A β due to enhanced transport of APP into the late secretory pathway. Moreover, our analysis showed remarkable production of p3-Alc α and Alc α ICD, which are the products of Alc α CTF following cleavage by γ -secretase. This observation indicates that *in vivo*, introduced Alc α CTF is quickly cleaved by γ -secretase to release Alc α ICD, which is free from membrane association. Indeed, *in vitro* experiments showed that Alc α ICD performs a novel function in releasing APP and Alc α from X11L, different from the function of membrane-associated Alc α and Alc α CTF.

Strikingly, both full-length APP and Alc α are released from X11L by excess expression of Alc α ICD in cultured cells. These studies *in vivo* and *in vitro* strongly indicate that Alc α ICD has different binding properties than full-length Alc α and may be a

Alc Fragment Regulates APP Trafficking and Metabolism

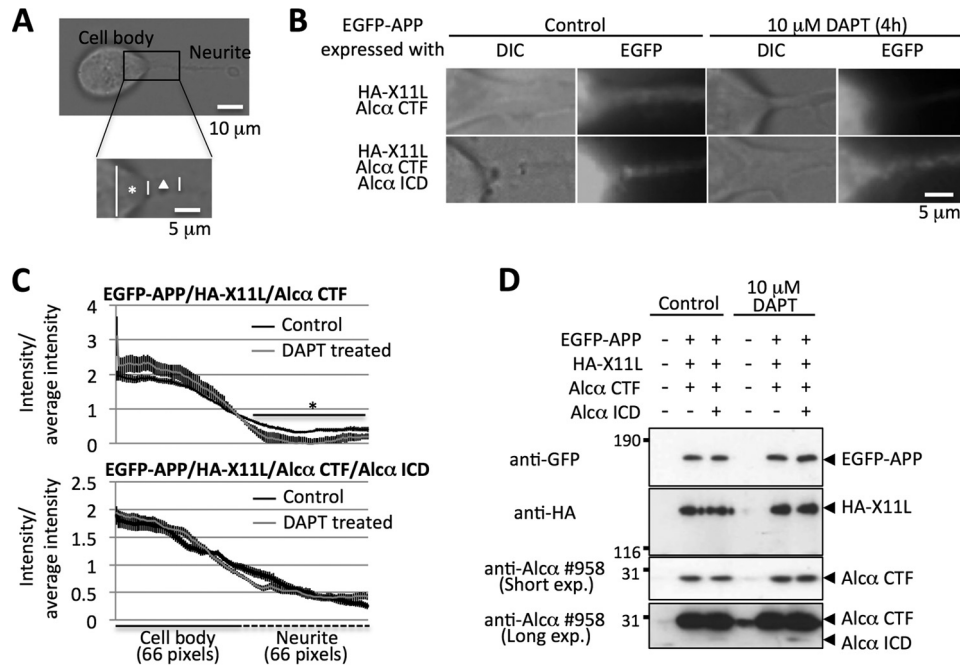


FIGURE 5. Alca ICD facilitates the trafficking of APP into neurites. *A*, the proximal region of neurites for analysis of APP trafficking. Neuro2a cells were observed under a transmission light and the hillock of cell body (asterisk, cell body) and the proximal region of neurite (triangle, neurite) were analyzed for EGFP-APP fluorescence as described under "Experimental Procedures." *B*, representative images of the fluorescence of EGFP-APP. The fluorescence of EGFP-APP was observed in living cells expressing HA-X11L and Alca CTF in the presence (top) or absence (bottom) of Alca ICD expression. Analyses were performed in the presence or absence of DAPT treatment (10 μM for 4 h). *C*, quantifications of fluorescence intensities of EGFP-APP at the proximal region of neurites. The intensities of EGFP-APP in *B* were quantified. The left panel indicates the intensity of cell body, and the right panel indicates the intensity of neurite. The fluorescence intensity of cell body or neurite is shown as a ratio to average intensity of cell body plus neurite. Black (control) and gray (DAPT-treated) lines are shown. The values are indicated with mean \pm S.E. ($n = 9-14$). *, $p < 0.05$, Student's *t* test. *D*, levels of protein expression in cells. Lysates of Neuro2a cells with or without DAPT treatment were analyzed by immunoblotting with anti-GFP no. 598 (MBL), anti-HA 12CA5 (Roche Applied Science), and anti-Alca 958 (for Alca CTF and Alca ICD) antibodies. Detected proteins are indicated with arrowheads. Transfection of plasmids is indicated with a plus sign, whereas a minus indicates the use of empty plasmid alone. Numbers indicate the protein molecular mass standards.

key molecule for the regulation of APP trafficking and metabolism. As shown in Figs. 2E and 4, we detected Alca ICD as a doublet. Interestingly, only the slower migrating band interacted with X11L in co-immunoprecipitation assays (Fig. 4). Although we determined that molecular weight of the faster migrating protein band was the expected size of hAlca ICD (data not shown), we have yet to identify the modification of slower-migrating protein band and determine why it interacts differently with X11L.

Several previous reports indicated that stalling of APP transport increases the production of A β because of the increased probability of association with secretases (36–38). The source of A β is still controversial. A recent report suggested that majority of intracellular APP is transported into lysosome from Golgi to generate A β (39). In contrast, it has been thought that cell surface APP is a significant source of A β (40, 41). Our observation that the increased A β in Tg mice brain is due to the increased synaptosomal APP level may be consistent with a hypothesis that cell surface APP contributes to the increased production of A β . We revealed here that increased trafficking of APP into the late secretory pathway facilitated APP metabolism, including A β generation, which was regulated by Alca ICD derived from Alca CTF by γ -secretase cleavage. Although the precise molecular mechanism is still under investigation, it is clear that dysfunctional APP intracellular trafficking is closely related to the aberrant production of A β . Moreover, the role of Alca ICD in the regulation of

membrane protein trafficking is a novel function of regulated intramembrane proteolysis.

REFERENCES

- Araki, Y., Tomita, S., Yamaguchi, H., Miyagi, N., Sumioka, A., Kirino, Y., and Suzuki, T. (2003) Novel cadherin-related membrane proteins, Alcadeins, enhance the X11-like protein mediated stabilization of amyloid β -protein precursor metabolism. *J. Biol. Chem.* **278**, 49448–49458
- Vogt, L., Schrimpf, S. P., Meskenaite, V., Frischknecht, R., Kinter, J., Leone, D. P., Ziegler, U., and Sonderegger, P. (2001) Calsyntenin-1, a proteolytically processed postsynaptic membrane protein with a cytoplasmic calcium-binding domain. *Mol. Cell Neurosci.* **17**, 151–166
- Hintsch, G., Zurlinden, A., Meskenaite, V., Steuble, M., Fink-Widmer, K., Kinter, J., and Sonderegger, P. (2002) The calsyntenins – a family of postsynaptic membrane proteins with distinct neuronal expression patterns. *Mol. Cell Neurosci.* **21**, 393–409
- Araki, Y., Kawano, T., Taru, H., Saito, Y., Wada, S., Miyamoto, K., Kobayashi, H., Ishikawa, H. O., Ohsugi Y., Yamamoto, T., Matsuno, K., Kinjo, M., and Suzuki, T. (2007) The novel cargo receptor Alcadein induces vesicle association of kinesin-1 motor components and activates axonal transport. *EMBO J.* **26**, 1475–1486
- Araki, Y., Miyagi, N., Kato, N., Yoshida, T., Wada, S., Nishimura, M., Komano, H., Yamamoto, T., De Strooper, B., Yamamoto, K., and Suzuki, T. (2004) Coordinated metabolism of Alcadein and amyloid β -protein precursor regulates FE65-dependent gene transactivation. *J. Biol. Chem.* **279**, 24343–24354
- Tomita, S., Ozaki, T., Taru, H., Oguchi, S., Takeda, S., Yagi, Y., Sakiyama, S., Kirino, Y., and Suzuki, T. (1999) Interaction of a neuron-specific protein containing PDZ domains with Alzheimer's amyloid precursor protein. *J. Biol. Chem.* **274**, 2243–2254
- Suzuki, T., and Nakaya, T. (2008) Regulation of amyloid β -protein precursor

- sor by phosphorylation and protein interactions. *J. Biol. Chem.* **283**, 29633–29637
8. Thinakaran, G., and Koo, E. (2008) Amyloid precursor protein trafficking, processing, and function. *J. Biol. Chem.* **283**, 29615–29619
 9. Konecna, A., Frischknecht, R., Kinter, J., Ludwig, A., Steuble, M., Meskenaite, V., Indermühle, M., Engel, M., Cen, C., Mateos, J. M., Streit, P., and Sonderegger, P. (2006) Calsyntenin-1 docks vesicular cargo to kinesin-1. *Mol. Biol. Cell* **17**, 3651–3663
 10. Hata, S., Fujishige, S., Araki, Y., Kato, N., Araseki, M., Nishimura, M., Hartmann, D., Saftig, P., Fahrenholz, F., Taniguchi, M., Urakami, K., Akatsu, H., Martins, R. N., Yamamoto, K., Maeda, M., Yamamoto, T., Nakaya, T., Gandy, S., and Suzuki, T. (2009) Alcadin cleavages by APP α - and γ -secretases generate small peptides p3-Alcs indicating Alzheimer disease-related γ -secretase dysfunction. *J. Biol. Chem.* **284**, 36024–36033
 11. Hata, S., Fujishige, S., Araki, Y., Taniguchi, M., Urakami, K., Peskind, E., Akatsu, H., Araseki, M., Yamamoto, K., Martins, R. N., Maeda, M., Nishimura, M., Levey, A., Chung, K. A., Montine, T., Leverenz, J., Fagan, A., Goate, A., Bateman, R., Holtzman, D. M., Yamamoto, T., Nakaya, T., Gandy, S., and Suzuki, T. (2011) Alternative γ -secretase processing of γ -secretase substrates in common forms of mild cognitive impairment and Alzheimer disease: Evidence for γ -secretase dysfunction. *Ann. Neurol.* **69**, 1026–1031
 12. Ludwig, A., Blume, J., Diep, T. M., Yuan, J., Mateos, J. M., Leuthäuser, K., Steuble, M., Streit, P., and Sonderegger, P. (2009) Calsyntenins mediate TGN exit of APP in a kinesin-1-dependent manner. *Traffic* **10**, 572–589
 13. Glabe, C. G. (2008) Structural classification of toxic amyloid oligomers. *J. Biol. Chem.* **283**, 29639–29643
 14. Benilova, I., Karran, E., and De Strooper, B. (2012) The toxic A β oligomer and Alzheimer's disease: an emperor in need of clothes. *Nat. Neurosci.* **15**, 349–357
 15. Piao, Y., Kimura, A., Urano, S., Saito, Y., Taru, H., Yamamoto, T., Hata, S., and Suzuki, T. (2013) Mechanism of intramembrane cleavage of Alcadin by γ -secretase. *PLoS One* **8**, e62431
 16. Saito, Y., Sano, Y., Vassar, R., Gandy, S., Nakaya, T., Yamamoto, T., and Suzuki, T. (2008) X11 proteins regulate the translocation of amyloid β -protein precursor (APP) into detergent-resistant membrane and suppress the amyloidogenic cleavage of APP by β -site-cleaving enzyme in brain. *J. Biol. Chem.* **283**, 35763–35771
 17. Saito, Y., Akiyama, M., Araki, Y., Sumioka, A., Shiono, M., Taru, H., Nakaya, T., Yamamoto, T., and Suzuki, T. (2011) Intracellular trafficking of the amyloid β -protein precursor (APP) regulated by novel function of X11-like. *PLoS One* **6**, e22108
 18. Lau, K. F., McLoughlin, D. M., Standen, C., and Miller, C. C. (2000) X11 α and X11 β interact with presenilin-1 via their PDZ domains. *Mol. Cell. Neurosci.* **16**, 557–565
 19. Lee, J. H., Lau, K. F., Perkinson, M. S., Standen, C. L., Rogelj, B., Falinska, A., McLoughlin, D. M., and Miller, C. C. (2004) The neuronal adaptor protein X11 β reduces amyloid β -protein levels and amyloid plaque formation in the brains of transgenic mice. *J. Biol. Chem.* **279**, 49099–49104
 20. Sano, Y., Nakaya, T., Pedrini, S., Takeda, S., Iijima-Ando, K., Iijima, K., Mathews, P. M., Itoharu, S., Gandy, S., and Suzuki, T. (2006) Physiological mouse brain A β levels are not related to the phosphorylation state of threonine 668 of Alzheimer APP. *PLoS One* **1**, e51
 21. Kondo, M., Shiono, M., Itoh, G., Takei, N., Matsushima, T., Maeda, M., Taru, H., Hata, S., Yamamoto, T., Saito, Y., and Suzuki, T. (2010) Increased amyloidogenic processing of transgenic human APP in X11-like deficient mouse brain. *Mol. Neurodegener.* **5**, 35
 22. Hogan, B., Bedding, R., Constantini, F., and Lacy E. (1986) *Manipulating the Mouse Embryo: A Laboratory Manual*, 2nd Ed., Cold Spring Harbor Laboratory Press, New York
 23. Nakaya, T., and Suzuki, T. (2006) Role of APP phosphorylation in Fe65-dependent gene transactivation mediated by AICD. *Genes Cells* **11**, 633–645
 24. Carlin, R. K., Grab, D. J., Cohen, R. S., and Siekevitz, P. (1980) Isolation and characterization of postsynaptic densities from various brain regions: enrichment of different types of postsynaptic densities. *J. Cell Biol.* **86**, 831–845
 25. Matsushima, T., Saito, Y., Elliott, J. L., Iijima-Ando, K., Nishimura, M., Kimura, N., Hata, S., Yamamoto, T., Nakaya, T., and Suzuki, T. (2012) Membrane-microdomain localization of amyloid β -precursor protein (APP) C-terminal fragments is regulated by phosphorylation of the cytoplasmic Thr668 residue. *J. Biol. Chem.* **287**, 19715–19724
 26. Konno, T., Hata, S., Hamada, Y., Horikoshi-Sakuraba, Y., Nakaya, T., Saito, Y., Yamamoto, T., Yamamoto, T., Maeda, M., Ikeuchi, T., Gandy, S., Akatsu, H., Suzuki, T., and Japanese Alzheimer's Disease Neuroimaging Initiative (2011) Coordinate increase of γ -secretase reaction products in the plasma of some female Japanese sporadic Alzheimer's disease patients: quantitative analysis with a new ELISA system. *Mol. Neurodegener.* **6**, 76
 27. Nakaya, T., Kawai, T., and Suzuki, T. (2008) Regulation of FE65 nuclear translocation and function by amyloid β -protein precursor in osmotically stressed cells. *J. Biol. Chem.* **283**, 19119–19131
 28. Brown, M. S., Ye, J., Rawson, R. B., and Goldstein, J. L. (2000) Regulated intramembrane proteolysis: a control mechanism conserved from bacteria to humans. *Cell* **100**, 391–398
 29. Morohashi, Y., and Tomita, T. (2013) Protein trafficking and maturation regulate intramembrane proteolysis. *Biochim. Biophys. Acta* **1828**, 2855–2861
 30. McLoughlin, D. M., Irving, N. G., Brownlee, J., Brion, J. P., Leroy, K., and Miller, C. C. (1999) Mint2/X11-like colocalizes with the Alzheimer's disease amyloid precursor protein and is associated with neuritic plaques in Alzheimer's disease. *Eur. J. Neurosci.* **11**, 1988–1994
 31. Xie, Z., Romano, D. M., and Tanzi, R. E. (2005) RNA interference-mediated silencing of X11 α and X11 β attenuates amyloid β -protein levels via differential effects on β -amyloid precursor protein processing. *J. Biol. Chem.* **280**, 15413–15421
 32. Ho, A., Liu, X., and Südhof, T. C. (2008) Deletion of Mint proteins decreases amyloid production in transgenic mouse models of Alzheimer's disease. *J. Neurosci.* **28**, 14392–14400
 33. Chaufy, J., Sullivan, S. E., and Ho, A. (2012) Intracellular amyloid precursor protein sorting and amyloid- β secretion are regulated by Src-mediated phosphorylation of Mint2. *J. Neurosci.* **32**, 9613–9625
 34. Saluja, I., Paulson, H., Gupta, A., and Turner, R. S. (2009) X11 α haploinsufficiency enhances A β amyloid deposition in Alzheimer's disease transgenic mice. *Neurobiol. Dis.* **36**, 162–168
 35. Mitchell, J. C., Ariff, B. B., Yates, D. M., Lau, K. F., Perkinson, M. S., Rogelj, B., Stephenson, J. D., Miller, C. C., and McLoughlin, D. M. (2009) X11 β rescues memory and long-term potentiation deficits in Alzheimer's disease APPswe Tg2576 mice. *Hum. Mol. Genet.* **18**, 4492–4500
 36. Kamal, A., Stokin, G. B., Yang, Z., Xia, C. H., and Goldstein, L. S. (2000) Axonal transport of amyloid precursor protein is mediated by direct binding to the kinesin light chain subunit of kinesin-I. *Neuron* **28**, 449–459
 37. Stokin, G. B., Lillo, C., Falzone, T. L., Brusch, R. G., Rockenstein, E., Mount, S. L., Raman, R., Davies, P., Masliah, E., Williams, D. S., and Goldstein, L. S. (2005) Axonopathy and transport deficits early in the pathogenesis of Alzheimer's disease. *Science* **307**, 1282–1288
 38. Almenar-Queralt, A., Falzone, T. L., Shen, Z., Lillo, C., Killian, R. L., Arreola, A. S., Niederst, E. D., Ng, K. S., Kim, S. N., Briggs, S. P., Williams, D. S., and Goldstein, L. S. (2014) UV irradiation accelerates amyloid precursor protein (APP) processing and disrupts APP axonal transport. *J. Neurosci.* **34**, 3320–3339
 39. Tam, J. H., Seah, C., and Pasternak, S. H. (2014) The amyloid precursor protein is rapidly transported from the Golgi apparatus to the lysosome and where it is processed into beta-amyloid. *Mol. Brain* **7**, 54
 40. Koo, E. H., and Squazzo, S. L. (1994) Evidence that production and release of amyloid beta-protein involves the endocytic pathway. *J. Biol. Chem.* **269**, 17386–17389
 41. Grbovic, O. M., Mathews, P. M., Jiang, Y., Schmidt, S. D., Dinakar, R., Summers-Terio, N. B., Ceresa, B. P., Nixon, R. A., and Cataldo, A. M. (2003) Rab5-stimulated up-regulation of the endocytic pathway increases intracellular β -cleaved amyloid precursor protein carboxyl-terminal fragment levels and A β production. *J. Biol. Chem.* **278**, 31261–31268